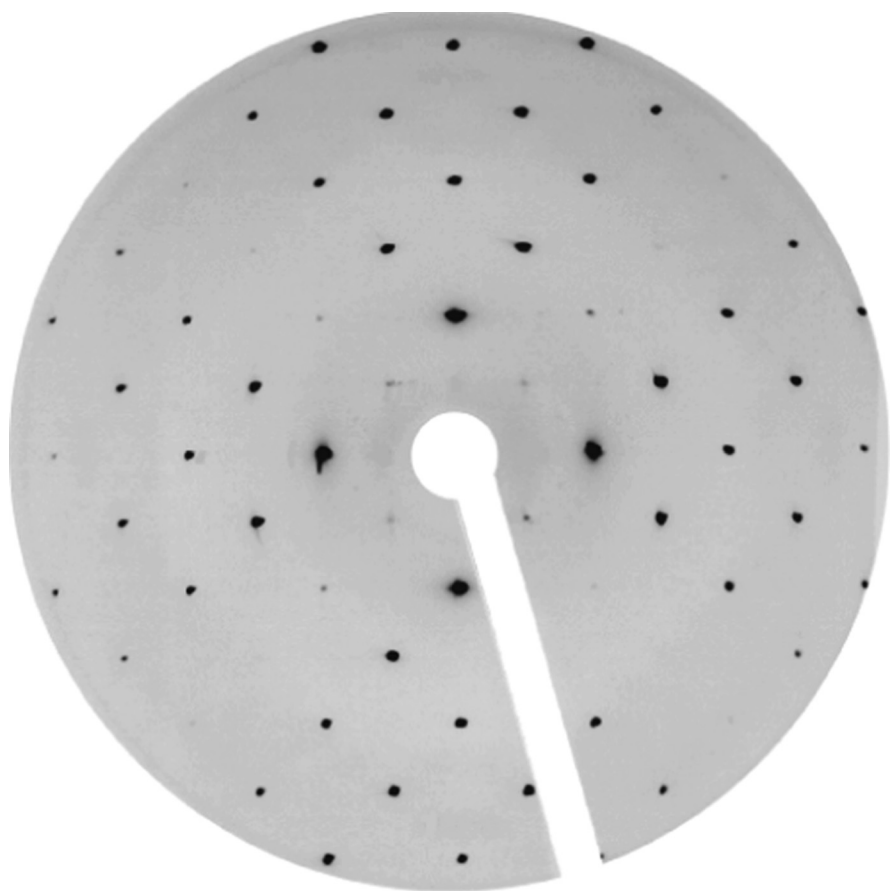


# Chapter 2

## Crystalline Solids: Diffraction

### Contents

2.1	Crystal Structures . . . . .	25
2.1.1	Crystal Lattice . . . . .	25
2.1.2	Two-Dimensional Crystals . . . . .	27
2.1.3	Three-Dimensional Crystals . . . . .	29
2.1.4	Beyond the Perfect Crystal . . . . .	33
2.2	Diffraction . . . . .	35
2.2.1	General Principles . . . . .	35
2.2.2	Reciprocal Lattice . . . . .	38
2.3	Determination of Crystal Structures . . . . .	39
2.3.1	On the Bragg Diffraction Condition . . . . .	39
2.3.2	Diffraction Intensity and Basis of the Primitive Cell . . . . .	41
2.3.3	X-Ray Diffraction . . . . .	42
2.4	Summary . . . . .	44
2.5	Answers to Questions . . . . .	45



X-ray diffraction pattern for a C<sub>60</sub> single crystal obtained with the experimental setup known as a precession chamber. This directly visualises the Bragg spots corresponding to a plane of the reciprocal lattice of the crystal (to solve Question 2.6 one has to take into account that the actual diameter of the film is 12 cm). Image courtesy of Launois, P., Moret, R.: Laboratoire de Physique des Solides, Orsay, France

Our main concern in this book is to describe the electronic properties of crystalline solids. The existence of translation symmetries associated with such ordered crystal structures leads to specific features in the electronic structure and to a specific representation of the energy states in wave vector space. In Sect. 2.1, we explain how a crystal structure can be described formally by defining a crystal lattice of non-material points together with a repeated material motif, known as the basis. This periodic structure of matter causes diffraction of electromagnetic waves, or equivalently, of quantum particles. We shall see in Sect. 2.2 that these diffraction phenomena lead to the notion of reciprocal lattice in wave vector space, and this will be important later for characterising the electronic states of these solids. In Sect. 2.3, we outline the experimental methods used to determine the crystal structures of solids using diffraction methods.

## 2.1 Crystal Structures

It is usual to consider a crystal as a natural object with regular external geometric features, as found for example in rock salt, diamonds, and so on. By the end of the nineteenth century, the systematic study of the external shapes of such natural crystals led scientists to conclude that this regularity of the outer faces must be due to structural regularities on the microscopic scale. The molecules or atoms had to be assembled in a periodic manner to make a crystal. In this chapter, we shall see how to specify the arrangement of a crystal structure. This structure can be ascertained experimentally either by direct observation, or by light diffraction (X-ray crystallography). These experimental methods show that many solids actually have a crystal structure, even when their outer surfaces do not give this impression. They are in fact polycrystalline, i.e., made up of a host of small crystals, which may themselves be of micrometric dimensions, but which are nevertheless of macroscopic size. We begin in Sect. 2.1.1 by describing the notions of crystal lattice and unit cell. In Sect. 2.1.2, these ideas will be exemplified in two dimensions, i.e., for planar crystal structures, where the geometric representations are simpler. We then illustrate some simple 3D systems in Sect. 2.1.3.

### 2.1.1 Crystal Lattice

A crystal is an arrangement of atoms or molecules that is invariant under translations in three space directions constituting a triad ( $\mathbf{a}_1, \mathbf{a}_2, \mathbf{a}_3$ ). Many human constructions have ordered structures exhibiting such characteristics, especially in two dimensions: wall paper and floor tiling often have periodic structures that can be considered as 2D crystals. In these cases, the primitive material basis is repeated through two translations. A molecular example, observed by a modern microscopic method, is shown in Fig. 2.1. These are alkane molecules with chemical formula

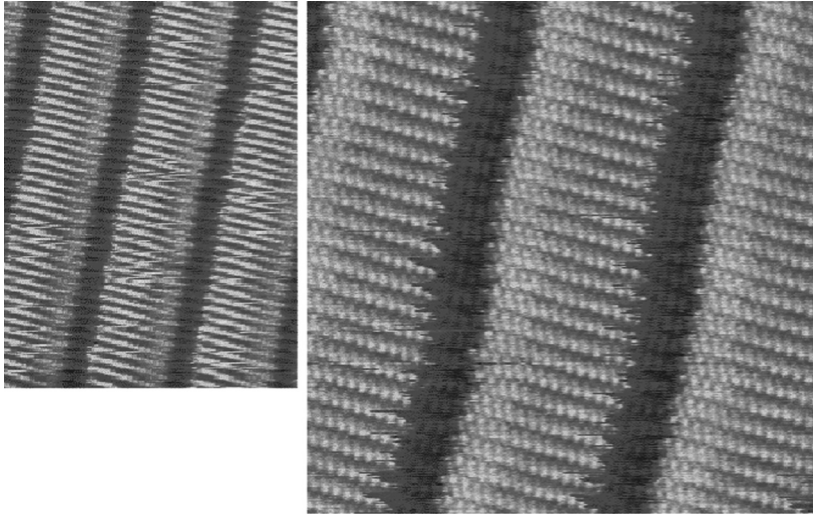


**Fig. 2.1** A monolayer of alkane  $C_{33}H_{68}$  deposited on graphite arranges itself into a 2D crystal. The right-hand figure was obtained with twice the resolution to reveal details of the atomic structure. The distance between molecules is  $4.5 \text{ \AA}$ , and their length is  $45 \text{ \AA}$ . Image courtesy of Cousty, J.: SPCSI/CEA. Saclay, France

$C_{33}H_{68}$ , deposited on a graphite surface. Note that, if we choose an origin  $O$  in space, the crystal can be reconstructed in two steps:

- We produce a lattice of points obtained from  $O$  by all the translations

$$\mathbf{R}_l = l_1 \mathbf{a}_1 + l_2 \mathbf{a}_2 + l_3 \mathbf{a}_3, \quad (2.1)$$

where  $l_1, l_2, l_3$  are integers. This set of points (the *lattice points* or *nodes*) constitutes the *crystal lattice* or *Bravais lattice*.

- In the second step, we arrange the material basis relative to these nodes in such a way as to completely tile the space.

The Bravais lattice is thus a set of non-material points, whereas the atoms and molecules make up the material basis, which we shall call the ‘basis’ from now on, when no confusion is possible. For elementary solids, containing only one atomic species, the atoms may coincide with the lattice nodes, since the basis then often comprises a single atom. But as soon as the solid contains several atomic species, such a situation is no longer possible.

Note that the lattice of points provides a way of defining a *primitive unit cell* for the material basis, namely, as the smallest volume that can tile the space by applying the translations  $\mathbf{R}_l$ . If  $n_p$  is the density of lattice points, the volume of the primitive cell is  $v = 1/n_p$ . The primitive cell and the triad  $(\mathbf{a}_1, \mathbf{a}_2, \mathbf{a}_3)$  are not unambiguously defined, as can be seen from Fig. 2.2. The triad  $(\mathbf{a}_1, \mathbf{a}_2, \mathbf{a}_3)$  is often taken to be the set of vectors that best reveals the symmetries of the lattice, e.g.,  $(\mathbf{a}_1, \mathbf{a}_2)$  rather than  $(\mathbf{b}_1, \mathbf{b}_2)$  for the square and rectangular planar lattices in Fig. 2.2. A primitive cell

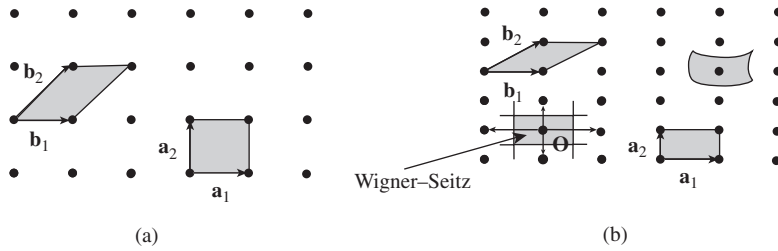


**Fig. 2.2** (a) *Square* lattice. (b) *Rectangular* lattice. These can be specified by the two vectors  $(\mathbf{a}_1, \mathbf{a}_2)$  or the two vectors  $(\mathbf{b}_1, \mathbf{b}_2)$ . The vectors  $(\mathbf{a}_1, \mathbf{a}_2)$  better reveal the symmetries of the lattice. Four primitive cells are shown for the *rectangular* lattice, those specified by  $(\mathbf{a}_1, \mathbf{a}_2)$  and  $(\mathbf{b}_1, \mathbf{b}_2)$ , an arbitrary cell, and the Wigner-Seitz cell containing the lattice point  $O$ . The latter is obtained by constructing the orthogonally bisecting planes of the four vectors  $(O\mathbf{a}_1, O\mathbf{a}_2, -O\mathbf{a}_1, -O\mathbf{a}_2)$

tiling the space may be chosen with an arbitrary shape as displayed in Fig. 2.2(b), but we often opt for the rhombohedral primitive cell specified by  $(\mathbf{a}_1, \mathbf{a}_2, \mathbf{a}_3)$ .

Of particular importance is a primitive unit cell known as the *Wigner-Seitz cell*. This is constructed in such a way that *every point of the cell is closer to one lattice point* (for example,  $O$ ) *than to any other lattice point* (see Fig. 2.2). It is bounded by the orthogonally bisecting planes of the vectors  $\mathbf{R}_i$  with origin the chosen node. For an elementary solid, this volume constructed with one atom at the center represents in some sense the region of influence of this atom.<sup>1</sup>

Note that the lattice points can be grouped together in parallel planes in infinitely many different ways. These are called *lattice planes*. In two dimensions, they constitute parallel rows (see Fig. 2.3). The lattice planes group together points that can be obtained from one another by two of the translations  $\mathbf{R}_i$ .

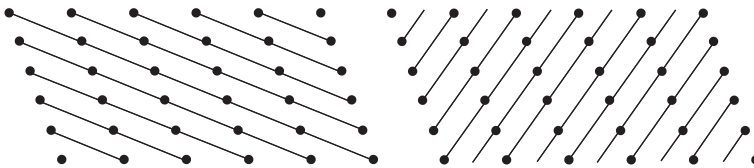


**Fig. 2.3** Two families of lattice rows in the same Bravais lattice (oblique lattice in a 2D space)

### 2.1.2 Two-Dimensional Crystals

In the above, we illustrated the idea of a crystal by 2D representations. Since real crystals are three-dimensional, these 2D representations may appear rather

<sup>1</sup> We shall see that, in the reciprocal lattice to be defined hereafter, the corresponding unit cell will specify the first Brillouin zone.

academic. However, important cases of 2D physics are becoming more and more common today:

- The surface of any 3D crystal is obviously a 2D structure. One might think that this would be that of the lattice plane corresponding to the infinite crystal. However, in many cases, the translational symmetry breaking associated with the existence of a surface leads to a significant modification of the surface structure. We refer to this as surface reconstruction.
- Many 3D crystals occur in a layered form, with widely spaced molecular or atomic layers. An example is graphite, or the high- $T_c$  cuprate superconductors. The structural and electronic properties of these materials are strongly affected by the 2D nature of the material.
- Finally, novel fabrication methods devised in nanotechnology are now used to deposit monomolecular layers (see Fig. 2.1), or even monatomic layers, on the surfaces of crystalline substrates. In 2004, it became possible to peel off graphite sheets and hence study isolated layers of graphene, which is an almost ideal 2D crystal form of carbon with highly original electronic properties.

Quite generally, a given (Bravais) crystal lattice is characterised by the symmetry operations that preserve its structure, and which include, apart from the lattice translations, axes of symmetry under rotation through some angle  $\theta$  (or  $n$ -fold symmetry axes, where  $\theta = 2\pi/n$ ), and planes of symmetry (*mirror planes*). In two dimensions, there are only five types of Bravais lattice. These are, in order of increasing symmetry:

- The oblique lattice (Fig. 2.3), which has the minimal 2D symmetry, i.e., only one two-fold symmetry axis perpendicular to the plane.
- The rectangular lattice (Fig. 2.2b), which also has mirror planes parallel to the shortest translation axes of the lattice.
- The centered rectangular lattice (see Fig. 2.4a), with mirror planes distinct from the shortest translation axes of the lattice.
- The hexagonal lattice (Fig. 2.4b), with a 3-fold (and hence a 6-fold) symmetry axis.
- The square lattice (Fig. 2.2a), with a 4-fold symmetry axis.

In the centered rectangular lattice of Fig. 2.4a, the primitive cell constructed from  $(\mathbf{a}_1, \mathbf{a}_2)$  does not help us to visualise the lattice symmetries as clearly as the *conventional unit cell*  $(\mathbf{a}, \mathbf{b})$ , which is not a primitive unit cell, since it has double the

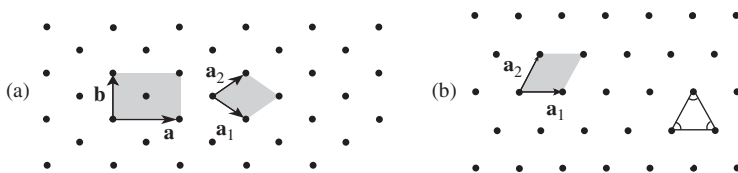


**Fig. 2.4** Plane lattices. (a) Centered *rectangular*, (b) *hexagonal*. In the first case, we observe the conventional centered *rectangular* cell specified by  $(\mathbf{a}, \mathbf{b})$  and the primitive cell  $(\mathbf{a}_1, \mathbf{a}_2)$ . In the plane *hexagonal* lattice, all the primitive *triangles* are equilateral

area. In fact the latter contains two lattice points, viz., the point at the origin and the center of the rectangle. These two points are indeed equivalent, as required by the notion of a Bravais lattice, since each one is the center of the rectangle formed by its four nearest neighbours. The conventional cell must be considered as a cell with one basis (the two lattice points), and the crystal will be obtained by introducing twice the material basis of the primitive cell around these points.

**Question 2.1.** 1. Determine the Bravais lattice and the primitive cell for the alkane crystal observed by scanning tunneling microscopy in Fig. 2.1.  
2. Determine the Wigner–Seitz cells associated with the centered rectangular and hexagonal lattices of Fig. 2.4.

The 2D structures attracting most attention since 2005 are the graphene honeycomb structure of Fig. 2.5a and the so-called Kagomé structure. Some compounds like hebersmithite  $\text{ZnCu}_3(\text{OH})_6\text{Cl}_2$  are built up from alternating planes of  $\text{ZnCl}_2$  with a simple 2D structure and Kagomé planes of  $\text{Cu}_3(\text{OH})_6$ . The  $\text{Cu}^{2+}$  ions are arranged as in Fig. 2.5b, while the  $(\text{OH})^-$  serve to bind the  $\text{Cu}^{2+}$ . The latter carry total electron spin  $1/2$ , making this a very interesting material in quantum magnetism.

**Question 2.2.** Determine the Bravais lattice and a primitive cell for each of the two structures of Fig. 2.5.

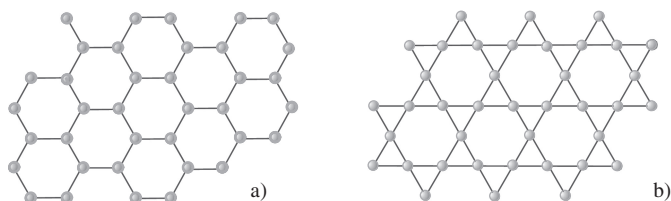


**Fig. 2.5** (a) Crystal structure of C atoms in graphene. (b) Atomic arrangement known as ‘Kagomé’ (after a typical pattern of straw baskets made in Japan)

### 2.1.3 Three-Dimensional Crystals

In three dimensions, the simplest lattice to visualise is the cubic lattice. The three primitive translation vectors ( $\mathbf{a}_1, \mathbf{a}_2, \mathbf{a}_3$ ) form an orthogonal triad, and each of them has length equal to the side  $a$  of the cube constituting a primitive cell (see Fig. 2.6a). Chemical elements crystallise scarcely into such a simple cubic lattice, but it is encountered in many polyatomic crystals (we shall discuss the example of CsCl below).

However, many chemical elements crystallise into body-centered cubic (bcc) crystal lattices (see Table 2.1). This Bravais lattice shown in Fig. 2.6b is the 3D

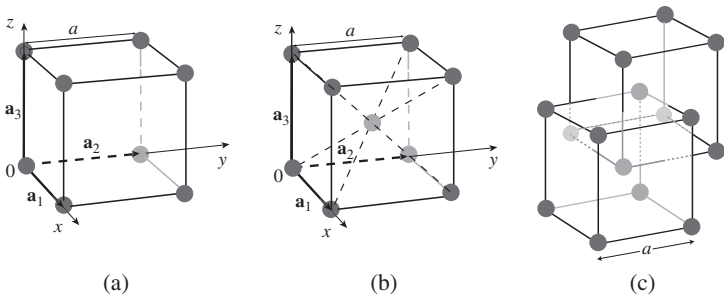


**Fig. 2.6** (a) Simple cubic lattice. (b) Body-centered cubic lattice. (c) Equivalence of nodes in the body-centered cubic lattice

**Table 2.1** Lattice constants  $a$  of the conventional cell for several elementary solids which form a body-centered cubic structure with one atom per primitive unit cell

Element	$a$ [Å]	Element	$a$ [Å]	Element	$a$ [Å]
Ba	5.02	Li	3.49	Ta	3.31
Cr	2.88	Mo	3.15	Tl	3.88
Cs	6.05	Na	4.23	V	3.02
Fe	2.87	Nb	3.30	W	3.16
K	5.23	Rb	5.59		

analog of the 2D centered rectangular lattice. In the bcc lattice, the conventional cell contains two lattice points, one at the origin and the other at the center of the cube. These two lattice nodes are indeed equivalent as each is the center of a cube formed by its eight nearest neighbours (see Fig. 2.6c).

The most common lattice for elementary solids is the face-centered cubic lattice (fcc). This is what is usually obtained when we try to stack hard spherical balls. It is a common structure for many metals (see Table 2.2). The face-centered

**Table 2.2** Lattice constants  $a$  of the conventional cell in several elementary solids which form face-centered cubic structures

Element	$a$ [Å]	Element	$a$ [Å]	Element	$a$ [Å]
Ar	5.26	Ir	3.84	Pt	3.92
Ag	4.09	Kr	5.72	Pu	4.64
Al	4.05	La	5.30	Rh	3.80
Au	4.08	Ne	4.43	Sc	4.54
Ca	5.58	Ni	3.52	Sr	6.08
Ce	5.16	Pb	4.95	Th	5.08
Co	3.55	Pd	3.89	Xe	6.20
Cu	3.61	Pr	5.16	Yb	5.49



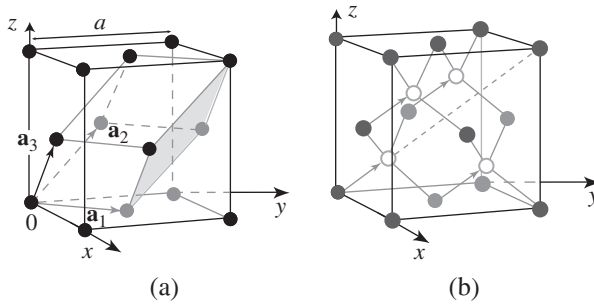


**Fig. 2.7** (a) Face-centered cubic lattice. The primitive cell is the rhombohedron specified by the vectors  $\mathbf{a}_1 = (a/2)(\mathbf{x} + \mathbf{y})$ ,  $\mathbf{a}_2 = (a/2)(\mathbf{y} + \mathbf{z})$ , and  $\mathbf{a}_3 = (a/2)(\mathbf{x} + \mathbf{z})$ . The conventional cell contains four lattice nodes. (b) Cubic crystal structure of diamond. The atoms are all chemically identical in diamond, Si, and Ge. In the case of InP or GaAs, the two species differ, and are represented by empty spheres and full spheres

cubic lattice also has a conventional cubic unit cell containing a four-node basis comprising one vertex of the cube and the three centers of the adjacent faces (see Fig. 2.7a). Note that the primitive translations of the Bravais lattice are the three vectors joining the cube vertex to the centers of the adjacent faces, so a rhombohedral primitive cell can be constructed (see Fig. 2.7a). Among the systems crystallising in this structure are diamond and many semiconductors such as Si, Ge, GaAs, and InP. All atoms within the conventional cell are shown in Fig. 2.7b, where the full and empty spheres correspond to the two atomic species in the case of binary compounds, but are identical in the case of Si or Ge.

**Question 2.3.** Check that the crystals in Fig. 2.7b do indeed correspond to a face-centered cubic Bravais lattice, and determine the atomic basis.

When we consider polyatomic crystals, the primitive cell necessarily contains several atoms. A simple illustration is given in Fig. 2.8 for the alkali halides CsCl and NaCl. Although Cs is at the center of a Cl cube, the associated Bravais lattice is the

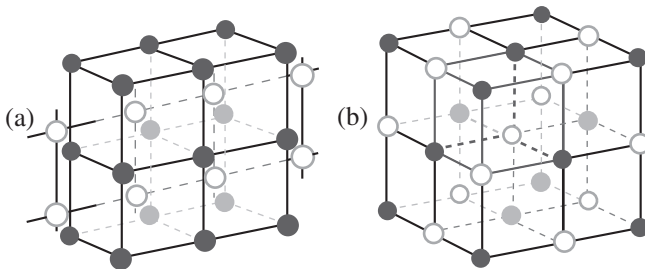


**Fig. 2.8** (a) Crystal of CsCl, with simple cubic primitive cell. The basis comprises one atom of Cl at the vertex of the cube and one atom of Cs at the center of the cube. (b) Crystal of NaCl with fcc primitive cell comprising one atom of Cl and one atom of Na per primitive cell of Fig. 2.7a

simple cubic lattice of side  $a$ , with a basis comprising one atom of Cl at the vertex of the cube and one atom of Cs at the center of the cube.

Many mixed oxides of transition metals crystallise into a cubic structure called the *perovskite structure*, with primitive cell  $\text{ABO}_3$ , in which A and B are cations with different size and valence. The small cation, generally  $\text{A}^{2+}$ , is surrounded by an octahedron of oxygen atoms, while the large cation  $\text{B}^{n+}$  (in general  $n = 3$  or 4) is surrounded by 12 oxygen atoms, as can be seen in Fig. 2.9a. These oxides can exhibit a wide range of physical properties, from ferromagnetism in the manganites  $\text{LaMnO}_3$  and cobaltites  $\text{LaCoO}_3$  to antiferromagnetism in iron-based perovskites like  $\text{LaFeO}_3$ . Below  $120^\circ\text{C}$ , slight structural distortions with respect to the ideal structure of Fig. 2.9a induce ferroelectric properties in the case of  $\text{BaTiO}_3$ .

Families of metal oxides with a highly 2D structure can sometimes be obtained by combining planes with perovskite structure with square MO planes, where M is a third metal cation. A classic example of such hybrid structures is provided by the high- $T_c$  cuprate superconductors, whose discoverers, Müller and Bednorz, were rewarded by the Nobel prize. An example of such a structure is found in  $\text{HgBa}_2\text{CuO}_5$ . This is shown in Fig. 2.9b. It is generated by intercalating sheets of  $\text{Ba}_2\text{CuO}_4$ , which has the perovskite structure, with planes of  $\text{HgO}$ , or can alternatively be considered simply as alternating planes of  $\text{CuO}_2/\text{BaO}/\text{HgO}/\text{BaO}/\text{CuO}_2$ , and so on. The primitive cell of this structure is a right-angled parallelepiped whose sides  $a$  and  $b$  are equal (tetragonal structure). In other cuprates with  $a \neq b$ , the structure is said to be orthorhombic.

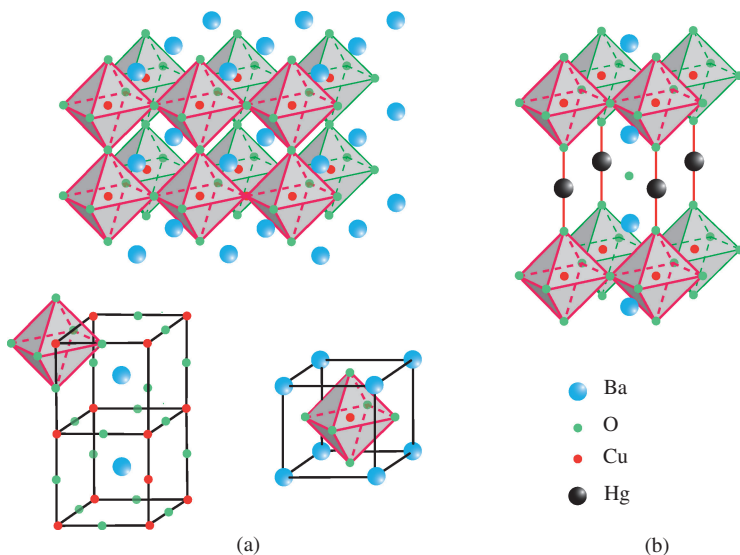


**Fig. 2.9** (a)  $\text{ABO}_3$  cubic perovskite structure. Below the 3D representation designed to show the octahedra surrounding the A cations are two primitive cells centered respectively on the A and B cations. (b) Quadratic structure of a high- $T_c$  cuprate superconductor made up of planes of  $\text{HgO}$  inserted between sheets of perovskite  $\text{Ba}_2\text{CuO}_4$ . This structure confers 2D physical properties on the material

Naturally, there are many other 3D crystal systems with even fewer symmetries than the simple lattices considered above. There is no question here of undertaking an exhaustive study: there are 14 Bravais lattices in three dimensions!

### 2.1.4 Beyond the Perfect Crystal

Not all natural or artificial solids are crystalline. In many cases, there is no long range order in the atomic arrangement. In particular, when a liquid is suddenly cooled down below its solidification temperature, we can obtain a solid state which simply freezes in the arrangement of atoms as it occurred in the liquid state. A glass is obtained in this way by quenching the liquid, whereupon the atoms arrange themselves in a way that suffers only one constraint, namely that atoms are not allowed to interpenetrate. If the atoms are thought of as hard spheres, the resulting glass structure looks like what would be obtained by putting beads in a container and shaking them up. This glassy state is generally metastable, in the sense that the system can have a lower free energy when the atoms are arranged into an fcc or hcp crystal structure, which correspond to the closest packing of the beads. Crystallisation can then be obtained by heat treatment, which amounts to shaking the box of beads in our analogy.

But many other situations can be observed, with varying degrees of order. Consider for example what happens for some *alloys* of two metals. A structure close to a crystal structure can often be seen in these materials. The atoms distribute themselves randomly at the lattice points of a perfect crystal structure. This is called a *solid solution*. This happens for example for the alloys  $\text{Au}_{1-x}\text{Cu}_x$ , which can be made with an arbitrary concentration  $x$  of Cu. The Cu and Au atoms distribute themselves randomly over the fcc lattice sites of pure Au, and the lattice spacing varies slightly depending on the Cu concentration. This structure is not strictly speaking a perfect crystal structure, although it can be treated as such in many respects.

**Question 2.4.** For some values of  $x$ , a heat treatment allows the atoms to arrange themselves into a perfect crystal structure on the lattice. In the case of the  $\text{Au}_{1-x}\text{Cu}_x$  alloys, indicate one or more values  $x_0$  of  $x$  for which a perfect arrangement could in principle be obtained. What would then be the associated primitive cell and Bravais lattice? In your opinion, if the  $\text{Au}_{1-x}\text{Cu}_x$  alloy forms a perfect crystal arrangement for  $x = x_0$ , is it likely from a physical point of view that the same arrangement will be obtained for  $x = 1 - x_0$ ?

Imperfect crystal arrangements are observed in many other cases, in particular for complex molecular structures. For example, the real crystals of cuprate superconductors shown in Fig. 2.9a are such that the HgO plane is highly deficient in oxygen. The chemical formula is then  $\text{HgBa}_2\text{CuO}_{4+\delta}$ , and the oxygen vacancies are important in determining the physical properties.

A novel illustration of disorder in crystals is shown below in the case of the fullerene  $\text{C}_{60}$ , a molecule discovered in 1985, which has a football shape. Its face-centered cubic structure, with large empty spaces between the  $\text{C}_{60}$  molecules,

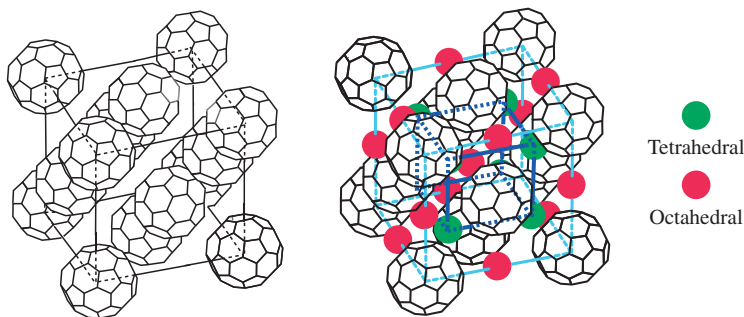


**Fig. 2.10** *Left:*  $C_{60}$  crystal. *Right:*  $Rb_3C_{60}$  crystal. These lattices are face-centered cubic. In  $Rb_3C_{60}$  the rhombohedral primitive cell contains a  $C_{60}$  molecule and three Rb atoms

is shown in Fig. 2.10. It is easy to insert cations between the  $C_{60}$  molecules and thereby create compounds of the form  $A_nC_{60}$ . The compound  $Rb_3C_{60}$  has attracted considerable attention as it happens to be a metal that becomes a superconductor below 27 K. Its fcc structure contains 3 rubidium atoms and one molecule of  $C_{60}$  per primitive cell. The rubidium atoms have two different types of position: one, located in the middle of an edge of the cube, has an octahedral  $C_{60}$  environment, while the other two have a tetrahedral  $C_{60}$  environment (one vertex of the cube and three face centers). Note that the  $C_{60}$  molecule has symmetries that are not compatible with the face-centered cubic lattice. Indeed, there is no way of orientating the  $C_{60}$  molecule so that it can map onto itself under all the symmetries of the lattice. There are not really any 3D crystal structures whose primitive cells are given by those shown in Fig. 2.10. These structures can nevertheless be considered as crystalline, but with orientational disorder of the  $C_{60}$  molecules.

### Crystals and Molecular Motions

At high temperatures, the  $C_{60}$  molecules are not immobile, but have rotational motions. These rapid rotational movements are such that, on average, the  $C_{60}$  molecules behave like spheres, and one can consider that the symmetry of the  $C_{60}$  molecule is no longer relevant. The average structure is as shown in Fig. 2.10, treating the  $C_{60}$  as simple spheres. Since the molecules are not fixed, we do not strictly have a crystal. Such systems in which molecular motions occur are called *plastic crystals*.

For pure  $C_{60}$ , a phase transition takes place at 260 K from the face-centered cubic high temperature structure of the plastic crystal to a body-centered cubic plastic crystal, as the rotational motions of the  $C_{60}$  molecules occur in a correlated manner about particular axes relative to the crystal axes.

At low temperatures, these rotational motions freeze, but the relative orientations of the  $C_{60}$  molecules in low temperature phases are not yet perfectly understood. Although one can speak of an average face-centered cubic structure in  $Rb_3C_{60}$ , the state of relative disorder or order of the  $C_{60}$  molecules has not yet been completely characterised.

## 2.2 Diffraction

In Sect. 2.2.1, we describe the general principles governing the diffraction of waves by a periodic pattern, and show that, for a crystal, the directions in which diffraction can occur are of course associated with the crystal structure. These diffraction conditions are used in Sect. 2.2.2 to define a lattice of points in the wave vector space, which is known as the *reciprocal lattice* of the crystal lattice.

### 2.2.1 General Principles

This effect was originally demonstrated by von Laue and the Braggs (father and son) in 1912–1913. The electromagnetic waves (photons) are generally X rays, with wavelength given in angstrom units ( $\text{\AA}$ ) and corresponding photon energy  $\varepsilon$  given in keV. The latter quantities are related by

$$\lambda_{\text{\AA}} = 12.4/\varepsilon_{\text{keV}} . \quad (2.2)$$

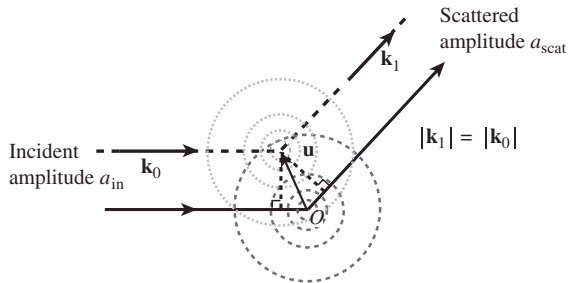
The X rays used typically have energies in the range  $10 < \varepsilon < 50$  keV. In specific cases, the radiation may also be in the form of neutrons or electrons. The wavelength is then given by the de Broglie relation  $\lambda = h/p$ .

To understand how diffraction works, consider first the scattering of an arbitrary plane (electromagnetic or matter) wave by some obstacle, usually an atom located at the origin (see Fig. 2.11). The amplitude of the incident wave will then have the form

$$a_{\text{in}}(\mathbf{r}, t) = a_0 e^{i(\mathbf{k}_0 \cdot \mathbf{r} - \omega t)} , \quad (2.3)$$

where  $\omega = c|\mathbf{k}_0|$  for an electromagnetic wave, with  $c$  the speed of light, and  $\omega = \hbar \mathbf{k}_0^2/2m$  for a matter wave, with  $m$  the mass of the incident particles. Here,  $a_0$  is a vector-valued amplitude in the case of electric or magnetic fields and a complex-valued amplitude in the case of quantum matter waves. This amplitude depends only on the intensity of the incident radiation. In general, the scattered wave will have the form

**Fig. 2.11** Scattering of an incident plane wave with wave vector  $\mathbf{k}_0$ . Waves scattered in the direction  $\mathbf{k}_1$  reveal the phase difference between beams scattered by two objects at  $0$  and  $\mathbf{u}$



$$a_{\text{scat}}(\mathbf{r}, t) = a_0 \sum_{\mathbf{k}} \alpha_{\mathbf{k}_0, \mathbf{k}} e^{i(\mathbf{k} \cdot \mathbf{r} - \omega t)}, \quad (2.4)$$

where conservation of energy implies that  $|\mathbf{k}| = |\mathbf{k}_0|$ . The determination of the coefficients  $\alpha_{\mathbf{k}_0, \mathbf{k}}$  is a (rather complex) problem of quantum mechanics which depends on the type of wave and the quantum properties of the scattering object. However, the exact expression for these coefficients is not needed to understand the underlying principle of the diffraction methods described below.

Let us now ask what happens when the object is displaced through  $\mathbf{u}$  from the origin. Clearly, the scattered amplitude must be taken from the point  $\mathbf{u}$  rather than from the origin. We must therefore replace  $\mathbf{u}$  by  $\mathbf{r} - \mathbf{u}$  in the exponential of the expression in (2.4). But in addition, the incident wave will have a phase offset of  $\mathbf{k}_0 \cdot \mathbf{u}$  (see Fig. 2.11), and we therefore obtain

$$a_{\text{scat}}(\mathbf{r}, t) = a_0 e^{i\mathbf{k}_0 \cdot \mathbf{u}} \sum_{\mathbf{k}} \alpha_{\mathbf{k}_0, \mathbf{k}} e^{i[\mathbf{k} \cdot (\mathbf{r} - \mathbf{u}) - \omega t]}. \quad (2.5)$$

Finally, we use a detector that only detects waves scattered in a specific direction  $\mathbf{k}_1$ . The amplitude in this specific direction will then be

$$a_{\text{scat}}(\mathbf{k}_1; \mathbf{r}, t) = a_0 \alpha_{\mathbf{k}_0, \mathbf{k}_1} e^{i(\mathbf{k}_1 \cdot \mathbf{r} - \omega t)} e^{-i\mathbf{K} \cdot \mathbf{u}}, \quad (2.6)$$

with

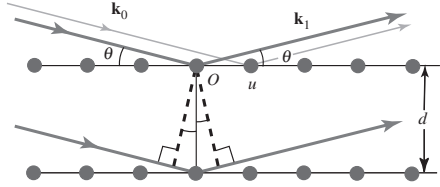
$$\mathbf{K} = \mathbf{k}_1 - \mathbf{k}_0. \quad (2.7)$$

There is therefore a phase difference between the waves scattered in the direction  $\mathbf{k}_1$  by the objects located at  $\mathbf{O}$  and  $\mathbf{u}$ . In the general case of a crystal where the identical scatterers are the material bases of the primitive cell repeated at the different lattice points, these scattered amplitudes will generally undergo different phase shifts  $\exp(i\mathbf{K} \cdot \mathbf{u})$ , leading to a low value of the total scattered intensity (sum of the squared amplitudes). However, as the Braggs and von Laue observed, if all the phase factors are the same in certain directions  $\mathbf{k}_1$ , the resulting *phase coherence* between the amplitudes scattered in these directions will lead to a high diffracted intensity.

### a. The Bragg Formulation

We consider the crystal lattice as an ensemble of lattice planes as shown in Fig. 2.12, with  $O$  and  $u$  two lattice points belonging to one of the lattice planes, and we take the scatterers to be the material bases of the primitive cell centered at  $O$  and  $u$ . If the wave vector  $\mathbf{k}_0$  of the incident wave makes an angle of incidence  $\theta$  with the lattice plane, it is easy to see that the phase difference  $\mathbf{K} \cdot \mathbf{u}$  vanishes if  $\mathbf{k}_1$  corresponds to a reflection of  $\mathbf{k}_0$  in the lattice plane. So in this direction, there will be phase coherence between the intensities scattered by all the bases associated with this

**Fig. 2.12** Reflection of incident radiation on lattice planes. The Bragg condition obtains when the path difference is a multiple of the wavelength



particular lattice plane. If in addition we wish to observe phase coherence between the amplitudes scattered by the different parallel lattice planes, examination of Fig. 2.12 shows that the condition that must be satisfied by  $\theta$  is

$$2d \sin \theta = n\lambda, \quad (2.8)$$

where  $d$  is the distance between the lattice planes and  $n$  is an integer. This diffraction condition, known as the *Bragg condition*, is given here in a form that corresponds to the representation of the crystal lattice in lattice planes.

## b. General von Laue Formulation

We now consider the scattering by a very large number of atomic bases of the primitive cell arranged in positions  $\mathbf{R}_n$ . The total scattered wave will simply be the superposition of many terms of the form (2.6):

$$a_{\text{scat}}^T(\mathbf{k}_1; \mathbf{r}, t) = a_0 e^{i(\mathbf{k}_1 \cdot \mathbf{r} - \omega t)} \mathcal{A}(\mathbf{K}), \quad (2.9)$$

with

$$\mathcal{A}(\mathbf{K}) = \alpha_{\mathbf{k}_0, \mathbf{k}_1} \sum_n e^{-i\mathbf{K} \cdot \mathbf{R}_n}. \quad (2.10)$$

In this equation,  $\alpha_{\mathbf{k}_0, \mathbf{k}_1}$  characterises the radiation and the arrangement of atoms in the primitive cell, while the sum over  $n$  is only associated with the spatial positions of the Bravais lattice points. If  $\mathbf{K}$  is chosen such that

$$e^{i\mathbf{K} \cdot \mathbf{R}_n} = 1, \quad \text{for all translation vectors } \mathbf{R}_n \text{ in the crystal lattice}, \quad (2.11)$$

we obtain  $\mathcal{A}(\mathbf{K}) = N\alpha_{\mathbf{k}_0, \mathbf{k}_1}$ , where  $N$  is the number of primitive cells in the crystal. Under these conditions, the diffracted intensity in the direction  $\mathbf{k}_1$  is

$$I_{\text{diff}} \propto |\mathcal{A}(\mathbf{K})|^2 = N^2 |\alpha_{\mathbf{k}_0, \mathbf{k}_1}|^2. \quad (2.12)$$

Equations (2.11) and (2.7) for  $\mathbf{k}_1$  and  $\mathbf{k}_0$  provide another expression of the *Bragg condition*.

### 2.2.2 Reciprocal Lattice

Here we interpret (2.11) in the special case of a linear chain. In one dimension, we have seen that the Bravais lattice is specified by  $\mathbf{R}_m = m\mathbf{a}_1 = max$ , where  $a$  is the period and  $\mathbf{x}$  a (dimensionless) unit vector along the  $Ox$  axis. The relation (2.11) implies that  $\mathbf{K}$  is an integer multiple of  $\mathbf{a}^* = (2\pi/a)\mathbf{x}$ .

In three dimensions, if  $\mathbf{K}$  is specified relative to a frame  $(\mathbf{a}_1^*, \mathbf{a}_2^*, \mathbf{a}_3^*)$  by

$$\mathbf{K} = x_1\mathbf{a}_1^* + x_2\mathbf{a}_2^* + x_3\mathbf{a}_3^*, \quad (2.13)$$

then (2.11) takes the form

$$(x_1\mathbf{a}_1^* + x_2\mathbf{a}_2^* + x_3\mathbf{a}_3^*)(l_1\mathbf{a}_1 + l_2\mathbf{a}_2 + l_3\mathbf{a}_3) = 2\pi n_l, \quad (2.14)$$

with  $n_l$  an integer, and this for all  $\mathbf{R}_l$ , i.e., for all integer values of  $(l_1, l_2, l_3)$ . We thus see that, by choosing the basis  $(\mathbf{a}_1^*, \mathbf{a}_2^*, \mathbf{a}_3^*)$  such that

$$\boxed{\mathbf{a}_i \cdot \mathbf{a}_j^* = 2\pi \delta_{ij}}, \quad (2.15)$$

the relation (2.14) reduces to

$$x_1 l_1 + x_2 l_2 + x_3 l_3 = n_l \text{ integer}, \quad (2.16)$$

and this for all  $(l_1, l_2, l_3)$ , implying that  $x_1, x_2$ , and  $x_3$  are also integers. The components of  $\mathbf{K}$  relative to the frame  $(\mathbf{a}_1^*, \mathbf{a}_2^*, \mathbf{a}_3^*)$  are called the *Miller indices*, and are usually denoted by  $(h, k, l)$ .

As a consequence, the vectors  $\mathbf{K}$  satisfying (2.11) generate a Bravais lattice in the  $\mathbf{k}$  space. This is the *reciprocal lattice* associated with the Bravais lattice in position space, called hereafter *real* or *direct*. The reference frame  $(\mathbf{a}_1^*, \mathbf{a}_2^*, \mathbf{a}_3^*)$  of the reciprocal space is defined in terms of the real space frame  $(\mathbf{a}_1, \mathbf{a}_2, \mathbf{a}_3)$  by (2.15). It is easy to check that the  $\mathbf{a}_i^*$  are given by

$$\boxed{\mathbf{a}_1^* = 2\pi \frac{\mathbf{a}_2 \wedge \mathbf{a}_3}{\mathbf{a}_1 \cdot (\mathbf{a}_2 \wedge \mathbf{a}_3)}}, \quad (2.17)$$

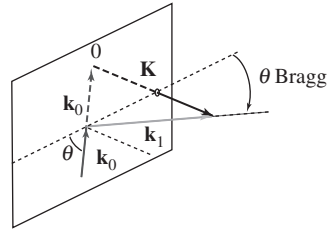
and cyclic permutations. Here the denominator is precisely the volume of the primitive cell of the direct lattice.

Note that, according to (2.11), the direct and reciprocal lattices play symmetric roles. In particular, the reciprocal lattice of the reciprocal lattice is just the direct lattice. However, the real crystal is a lattice of atoms or molecules, or more generally, a lattice of what we have called material bases, whereas the reciprocal lattice is a *lattice of points that are independent of the bases of the real crystal*.

For example, the reciprocal lattice of a simple cubic lattice with lattice constant  $a$  is a simple cubic lattice with lattice constant  $2\pi/a$ . The reciprocal lattice of an fcc lattice with lattice constant  $a$  is a body-centered cubic lattice of lattice constant  $4\pi/a$ , e.g., Al, Si, GaAs. Conversely, the reciprocal lattice of a body-centered cubic lattice is an fcc lattice, e.g., Fe.



**Fig. 2.13** Determination of the Bragg plane



The notion of reciprocal lattice can be used to relate the Bragg and von Laue representations of the diffraction conditions. Indeed, since  $|\mathbf{k}_0| = |\mathbf{k}_1|$ , the diffraction condition  $\mathbf{k}_1 - \mathbf{k}_0 = \mathbf{K}$  implies that

$$2\mathbf{k}_1 \cdot \mathbf{K} = K^2. \quad (2.18)$$

As illustrated in Fig. 2.13, this means that  $\mathbf{k}_0$  and  $\mathbf{k}_1$  are obtained from one another by a reflection in the orthogonally bisecting plane of the vector  $\mathbf{K}$ . The direction of diffraction  $\mathbf{k}_1$  therefore corresponds to a Bragg diffraction on the lattice planes of the crystal parallel to the orthogonally bisecting plane of the vector  $\mathbf{K}$ . There is thus a one-one correspondence between the lattice planes of the crystal and the orthogonally bisecting planes of the reciprocal lattice vectors, which are known conventionally as *Bragg planes*.

## 2.3 Determination of Crystal Structures

In Sect. 2.3.1, we show to begin with that the directions satisfying the Bragg condition are well defined experimentally, but that they are not always easy to detect. Once they have been found, the crystal lattice can be determined. In Sect. 2.3.2, we describe how the basis of the primitive cell can be ascertained by determining the intensities of the different Bragg diffraction spots. This will be exemplified for the case of X-ray diffraction in Sect. 2.3.3.

### 2.3.1 On the Bragg Diffraction Condition

We have seen that the diffracted intensity is high when the factor

$$A_0(\mathbf{K}) = \sum_n e^{-i\mathbf{K} \cdot \mathbf{R}_n}$$

is large, and this occurs when the Bragg condition holds:

$$\boxed{\mathbf{k}_1 - \mathbf{k}_0 = \mathbf{K}, \quad \mathbf{K} \in \text{reciprocal lattice}}. \quad (2.19)$$

Consider now the scattered intensity if the Bragg condition is not satisfied. To simplify the notation, we discuss the case of a simple cubic structure with lattice constant  $a$  and length  $La$  in each of the three space directions. The sum in (2.10) then becomes the product of three geometric sums, and direct calculation gives

$$|\mathcal{A}(\mathbf{K})|^2 = |\alpha_{\mathbf{k}_0, \mathbf{k}_1}|^2 f(K_x a) f(K_y a) f(K_z a), \quad \text{with} \quad f(x) = \frac{\sin^2 \frac{xL}{2}}{\sin^2 \frac{x}{2}}, \quad (2.20)$$

where  $\mathbf{K}$  is not a reciprocal lattice vector here. Figure 2.14 shows  $f(x)$  for two values of  $L$ . We observe that, apart from the Bragg diffraction points  $2n\pi$ , where  $\mathbf{K}$  is a reciprocal lattice vector, this function remains small everywhere. *If the Bragg condition is not satisfied, the scattered intensity will therefore remain very low.* However, the maxima at points  $x = 2n\pi$  become sharper and sharper as  $L$  increases, which supports the result (2.12). We thus conclude that the diffraction conditions are very precisely specified, and this will only be limited experimentally by the size of the diffracting crystal and the wavelength dispersion of the incident radiation.

**Question 2.5.** For the alloy  $\text{Cu}_{1-x}\text{Au}_x$  of Question 2.4, how does the diffraction pattern change when the Cu and Au atoms arrange themselves for the concentration  $x_0$ ?

To determine the reciprocal lattice, and hence the Bravais lattice, it remains only to determine all the space directions in which Bragg diffraction occurs. Experimentally, it is not totally obvious how to determine the directions in which Bragg diffraction will occur. This is illustrated in Fig. 2.15a, which shows the *Ewald construction*, used to determine the diffraction directions for an incident wave  $\mathbf{k}_0$  and a given position of the crystal. The points of the reciprocal lattice corresponding to this position of the crystal are shown in the left-hand figure, taking the origin  $\Gamma$  of the reciprocal lattice to be the point corresponding to the end of the vector  $\mathbf{k}_0$ . The diffraction directions are obtained by determining the points of the reciprocal lattice on a sphere, known as the Ewald sphere, with radius  $|\mathbf{k}_0|$  and centered at the

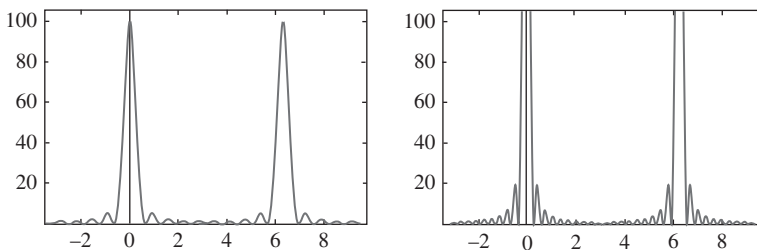


**Fig. 2.14** The function  $f(x)$  for  $x$  between  $-\pi$  and  $3\pi$ . *Left:*  $L = 10$ . *Right:*  $L = 20$ . Note that, on the right-hand graph, the peak is at the ordinate value 400

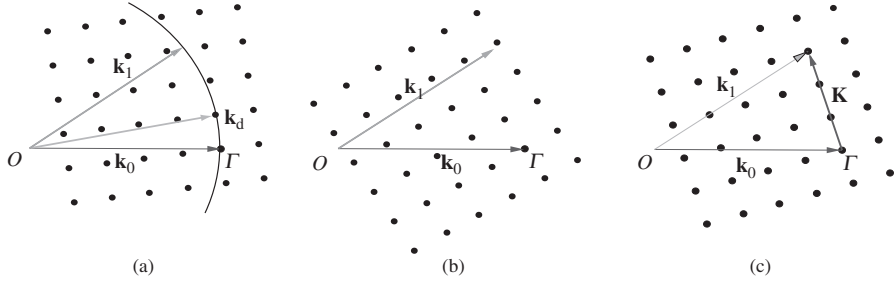


**Fig. 2.15** Geometry of Bragg diffraction in reciprocal space. For an incident vector  $\mathbf{k}_0$ , diffraction directions such as  $\mathbf{k}_d$  are obtained using the Ewald construction as shown in (a). The reciprocal lattice with origin  $\Gamma$  is depicted. For an incident vector  $\mathbf{k}_0$  and a detector in the direction  $\mathbf{k}_1$ , no Bragg diffraction will generally be detected (b), except for certain specific orientations of the crystal, such that the associated reciprocal lattice is oriented as shown in (c), for example

origin  $O$  of  $\mathbf{k}_0$ . Diffraction directions such as  $\mathbf{k}_d$  which join  $O$  to these points of the reciprocal lattice are few and far between.

If we have only one detector set in the direction  $\mathbf{k}_1$ , for example, there will generally be little diffraction in this direction. If the crystal is then rotated in space, according to (2.17), the reciprocal space will also rotate about its origin  $\Gamma$ . As can be seen from Fig. 2.15, Bragg diffraction will only be detected in the given direction  $\mathbf{k}_1$  for very specific orientations of the crystal. Given that we are working in 3D space, it is clear that, for a randomly chosen orientation of the crystal relative to the incident radiation, we will only very rarely observe a Bragg diffraction peak (or spot).

There are several experimental methods to get round this difficulty, e.g., using powders rather than single crystals, but we shall not discuss the issue further here. Knowing the orientations at which diffraction occurs, we may then characterise the reciprocal lattice, and hence also the crystal symmetries and the size of the primitive cell in the crystal lattice itself.

### 2.3.2 Diffraction Intensity and Basis of the Primitive Cell

So far we have not considered the structure of the diffracting object in any detail. Suppose now that we observe the diffraction by a crystal whose primitive cell comprises  $N_a$  atoms, possibly of different chemical nature, at positions  $\mathbf{r}_l$  inside the unit cell. In this case, a coefficient  $\alpha_{\mathbf{k}_0, \mathbf{k}_1}^{(l)}$  is associated with each atom. The sum in (2.9) over all sites  $l$  leads to a diffracted amplitude in the direction  $\mathbf{k}_1$  given by

$$\mathcal{A}(\mathbf{K}) = \sum_{l=1}^{N_a} \alpha_{\mathbf{k}_0, \mathbf{k}_1}^{(l)} \sum_n e^{-i\mathbf{K} \cdot (\mathbf{R}_n + \mathbf{r}_l)} = \left[ \sum_{l=1}^{N_a} \alpha_{\mathbf{k}_0, \mathbf{k}_1}^{(l)} e^{-i\mathbf{K} \cdot \mathbf{r}_l} \right] \left( \sum_n e^{-i\mathbf{K} \cdot \mathbf{R}_n} \right). \quad (2.21)$$

There are thus two multiplicative factors in the expression for the diffracted intensity. One of these,

$$\mathcal{A}_0(\mathbf{K}) = \sum_n e^{-i\mathbf{K} \cdot \mathbf{R}_n},$$

depends only on the Bravais lattice of the crystal and is only nonzero when the Bragg condition (2.19) is satisfied. The second,

$$S(\mathbf{K}) = \sum_{l=1}^{N_a} \alpha_{\mathbf{k}_0, \mathbf{k}_1}^{(l)} e^{-i\mathbf{K} \cdot \mathbf{r}_l}, \quad (2.22)$$

called the *structure factor*, depends only on the basis of the primitive cell and the nature of the diffracted radiation through the coefficients  $\alpha_{\mathbf{k}_0, \mathbf{k}_1}^{(l)}$ . If we measure the intensities of many Bragg diffraction spots, we can then deduce the structure of the primitive cell, provided we have a good understanding of the physical processes involved in the scattering of radiation by the atoms, since it is these processes that determine the values of the coefficients  $\alpha_{\mathbf{k}_0, \mathbf{k}_1}^{(l)}$ . Note that these coefficients will be different for X-ray diffraction, the X rays being scattered by electrons, and neutron diffraction, since neutrons are scattered by the atomic nuclei.

### 2.3.3 X-Ray Diffraction

In the specific case of X-ray diffraction, the coefficients  $\alpha_{\mathbf{k}_0, \mathbf{k}_1}$  can be expressed very simply by considering the underlying physical process for the scattering of X rays by atoms. Indeed, at the high frequencies associated with X rays, the electric field of the electromagnetic wave couples predominantly with the electrons in the atom. Each electron vibrates in phase with the incident wave at its frequency  $\omega$ . The electron charge thus has an oscillatory motion with angular frequency  $\omega$ , and consequently emits an electromagnetic wave at this same angular frequency, in phase with the incident wave.

Consider an atom centered at the origin  $O$  and with electronic density distribution  $\rho(\mathbf{u})$ , where  $\mathbf{u}$  indicates the position of an electron relative to  $O$ . The amplitude of the wave scattered in the direction  $\mathbf{k}_1$  by the electronic density at  $O$  is proportional to the electronic density at this point:

$$a_0 \rho(\mathbf{0}) e^{i(\mathbf{k}_1 \cdot \mathbf{r} - \omega t)}. \quad (2.23)$$

Consider now an arbitrary point at position  $\mathbf{u}$ . In an analogous way to Fig. 2.11, the amplitude scattered in the direction  $\mathbf{k}_1$  can thus be written

$$a_0 \rho(\mathbf{u}) e^{i[\mathbf{k}_1 \cdot (\mathbf{r} - \mathbf{u}) - \omega t]} e^{i\mathbf{k}_0 \cdot \mathbf{u}}. \quad (2.24)$$

The total wave diffracted in the direction  $\mathbf{k}_1$  by all the electrons in the atom is therefore

$$a_{\text{diff}}(\mathbf{k}_1, \mathbf{r}) = a_0 e^{i(\mathbf{k}_1 \cdot \mathbf{r} - \omega t)} \int \rho(\mathbf{u}) e^{-i(\mathbf{k}_1 - \mathbf{k}_0) \cdot \mathbf{u}} d^3 \mathbf{u}, \quad (2.25)$$

where  $|\mathbf{k}_1| = |\mathbf{k}_0|$ . This expression, valid for any molecular ensemble of electronic density  $\rho(\mathbf{u})$ , shows that *the diffraction amplitude of the X rays is directly related to the Fourier transform of the electronic density*. The diffraction pattern produced by an arbitrary object thus contains information about the structure of the diffracting object.

Going back to the case of a single atom and comparing (2.25) and (2.6), we define the *atomic form factor*

$$\alpha_{\mathbf{k}_0, \mathbf{k}_1} = \int \rho(\mathbf{u}) e^{-i(\mathbf{k}_1 - \mathbf{k}_0) \cdot \mathbf{u}} d^3 \mathbf{u} = f(\mathbf{k}_1 - \mathbf{k}_0). \quad (2.26)$$

For a crystal whose primitive cell contains  $N_a$  atoms at position  $\mathbf{r}_l$ , the diffraction amplitude is the Fourier transform of the total electronic density, which is the periodic reproduction of the electronic density of the primitive cell. The latter is given by (2.21), where the structure factor is simply

$$S(\mathbf{K}) = \sum_{l=1}^{N_a} f_l(\mathbf{K}) e^{-i\mathbf{K} \cdot \mathbf{r}_l}. \quad (2.27)$$

It can be determined once we know the form factors and the positions of the different atoms in the primitive cell. We thus find that the experimental determination of the intensities of the Bragg diffraction peaks or spots will be extremely useful for ascertaining the arrangement of atoms in the primitive cell of the Bravais lattice.

Let us consider a specific example to illustrate how the basis of the primitive cell affects the intensity of the Bragg peaks. Consider X-ray diffraction by a crystal of  $C_{60}$  whose fcc primitive cell is shown in Fig. 2.10. A suitable experimental setup records on a photographic film all the diffraction spots corresponding to the vectors  $\mathbf{K}$  in one plane of reciprocal space (see the image on p. 24). The pattern observed can thus be used to directly visualise a plane of the reciprocal lattice and its symmetries. In the image on p. 24, the spots are such that the vectors  $\ell_K$  separating them correspond to the vectors  $\mathbf{K}$  in one plane of the reciprocal lattice up to a scale factor given by  $|\mathbf{K}| = 2\pi |\ell_K| / \lambda L$ . Here  $\lambda$  is the wavelength of the X rays and  $L$  is a length depending on the experimental setup. (Here  $\lambda = 1.542 \text{ \AA}$  and  $L = 0.06 \text{ m}$ .)

- Question 2.6.** 1. Identify the body-centered cubic reciprocal lattice plane visualised in the image of p. 24. Deduce the dimensions of the primitive cell for  $C_{60}$ .
2. Some of the diffraction spots are very faint. Which vectors of the reciprocal lattice do these correspond to? To understand this, we take into account the fact that the X rays are scattered by electrons. We may consider the  $C_{60}$  molecule as a uniform charge distribution  $p(r)$  over the surface of a hollow sphere of radius  $R_0$ , viz.,  $p(r) = A\delta(r - R_0)$ . Calculate the structure factor for the  $C_{60}$  crystal. Deduce the radius  $R_0$  of  $C_{60}$ .

This aspect of X-ray diffraction was very important in determining the spatial structure of complex molecules, such as biological molecules, which are commonly conserved in solution. By crystallising  $N$  molecules, one then benefits from the fact that, in a crystal, the Bragg diffraction spots have intensities that increase as  $N^2$ , whereas the intensity only increases as  $N$  when the molecules do not have a crystalline arrangement. This method was used to determine the structure of DNA and many other biologically important molecules.

Note that disorder or atomic and molecular motions modify the intensities of the Bragg diffraction spots. The effect of lattice vibrations is discussed in Problem 1: *Debye–Waller factor*.

## 2.4 Summary

A crystal lattice can be described as a combination of two entities: the Bravais lattice, which is a periodic arrangement of lattice points in space, and hence an abstract construction, and a material basis which is the actual physical entity associated with each node of the Bravais lattice. These are given by

$$\mathbf{R}_\ell = \ell_1 \mathbf{a}_1 + \ell_2 \mathbf{a}_2 + \ell_3 \mathbf{a}_3 ,$$

where  $(\mathbf{a}_1, \mathbf{a}_2, \mathbf{a}_3)$  is a vector basis specifying a primitive cell of the lattice. In the simplest cases, the material basis is a single atom, but it may be a much more complex physical entity, such as an arrangement of atoms, one or more molecules, and so on.

The structures of arbitrary molecular entities can be determined using diffraction methods. An incident wave of wave vector  $\mathbf{k}_0$  is elastically scattered by the various objects making up the molecular entity. Interference between the scattered waves leads to a diffraction pattern. In the case of a crystal, the diffracted intensity is only significant in specific directions  $\mathbf{k}_1$  satisfying

$$\mathbf{k}_1 - \mathbf{k}_0 = \mathbf{K} ,$$

where  $\mathbf{K}$  is a vector belonging to another lattice called the reciprocal lattice for the actual lattice in real space. This relation is the Bragg diffraction condition.

The vectors  $\mathbf{K}$  of the reciprocal lattice are defined by the condition

$$e^{i\mathbf{K} \cdot \mathbf{R}_\ell} = 1 ,$$

for any  $\mathbf{R}_\ell$  belonging to the Bravais lattice of the crystal. The reference triad  $(\mathbf{a}_1^*, \mathbf{a}_2^*, \mathbf{a}_3^*)$  of the reciprocal lattice is given by

$$\mathbf{a}_1^* = 2\pi \frac{\mathbf{a}_2 \wedge \mathbf{a}_3}{(\mathbf{a}_1 \cdot \mathbf{a}_2 \wedge \mathbf{a}_3)} ,$$

and cyclic permutations. The vectors  $\mathbf{k}_1$  satisfying the Bragg diffraction condition can be used to determine the reciprocal lattice. The amplitude of the diffraction is related to the basis of the primitive cell of the crystal. It is given by

$$A(\mathbf{K}) = S(\mathbf{K}) \sum_n e^{-i\mathbf{K} \cdot \mathbf{R}_n},$$

where  $S(\mathbf{K})$  is the structure factor of the basis of the crystal.

For X rays, scattering is due to electrons in the atomic orbitals, and each atom  $l$  at  $\mathbf{r}_l$  is characterised by its atomic structure factor  $f_l(\mathbf{k}_1 - \mathbf{k}_0)$ . The structure factor of the primitive cell is then

$$S(\mathbf{K}) = \sum_{l=1}^{N_a} f_l(\mathbf{K}) e^{-i\mathbf{K} \cdot \mathbf{r}_l}.$$

## 2.5 Answers to Questions

### Question 2.1

1. The alkane molecules are arranged in parallel rows. Note that two consecutive rows are staggered in a quincuncial arrangement. This is checked by looking at Fig. 2.1 at grazing incidence with respect to the axis of the molecules. The lattice is therefore centered rectangular. Figure 2.16 shows the centered rectangular conventional unit cell ( $\mathbf{a}, \mathbf{b}$ ) and the primitive unit cell ( $\mathbf{a}_1, \mathbf{a}_2$ ) containing one alkane molecule. This is shown on part of the image and also on a molecular model.
2. It is an irregular polyhedron for the centered rectangular lattice and a hexagon for the hexagonal lattice (see Fig. 2.17).

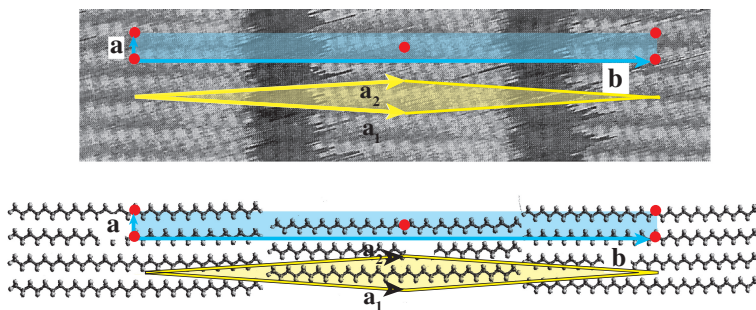


**Fig. 2.16** Centered rectangular cell and primitive unit cell for the 2D alkane crystal of Fig. 2.1. These are shown on an enlarged portion of the image of Fig. 2.1 (*upper*) and on a molecular model (*lower*)

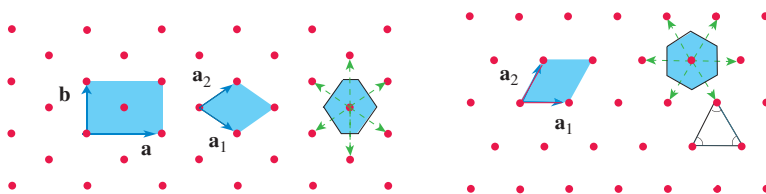


**Fig. 2.17** First Brillouin zones of the centered rectangular and hexagonal 2D lattices: construction displayed *on the right* for each reciprocal lattice

## Question 2.2

The honeycomb structure of graphene corresponds to a hexagonal lattice in which one in three sites have been removed. The primitive cell ( $\mathbf{a}_1, \mathbf{a}_2$ ) is hexagonal with three times the area of the initial hexagonal cell, i.e.,  $3a^2\sqrt{3}/2$ . It contains two carbon atoms placed at the nodes of two hexagonal sublattices of types A and B, which differ in the opposite orientations of their nearest neighbours. Each atom A has three nearest neighbours B and vice versa.

The Kagomé plane structure corresponds to a hexagonal lattice in which one site in four has been removed (one site out of two and in one line out of two). Its Bravais lattice is hexagonal with twice the lattice constant of the initial structure. The primitive cell contains 3 atoms of  $\text{Cu}^{2+}$  and 6  $(\text{OH})^-$  (see Fig. 2.18).

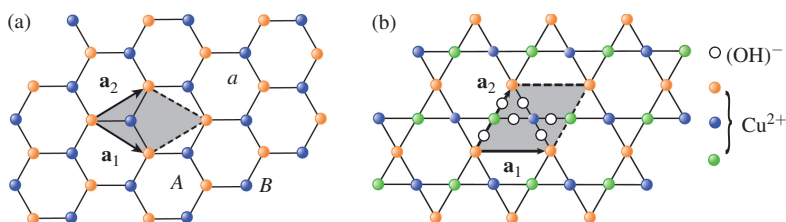


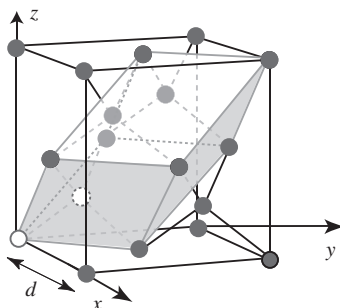
**Fig. 2.18** Unit cell and bases of the Bravais lattices for the graphene sheet and for the Kagomé 2D planes of the hebersmithite crystal

## Question 2.3

The crystal in Fig. 2.7b corresponds to an fcc lattice with full spheres at the lattice points and empty spheres obtained from the full ones by translation through  $(a/4, a/4, a/4)$ . There are thus two atoms per polyhedral primitive cell in Fig. 2.7a, shown by two empty spheres in Fig. 2.19, one at the corner of the cube and the other at  $(a/4, a/4, a/4)$ . There are 8 atoms per fcc unit cell: the vertex, the three centers of adjacent faces, and the 4 empty spheres in Fig. 2.7b.



**Fig. 2.19** Primitive unit cell of the diamond structure. The atoms located on the two empty spheres represent the basis for this crystal



### Question 2.4

When the atoms  $\text{Au}_{1-x}\text{Cu}_x$  are randomly distributed over the sites of the fcc Bravais lattice, the crystal structure is not perfect. The atoms must be placed at the sites of the fcc lattice in a periodic manner to obtain a perfect arrangement. With two different atoms, viz., Cu and Au, the primitive cell of the perfect crystal will have at least one two-atom basis and hence a Bravais lattice with unit cell at least doubled in volume.

It should be fairly clear that it is not possible to associate the sites of the fcc structure two by two to define a new Bravais lattice. However, if we take 4 atoms with 3 the same, one of the atoms can be placed at the vertex of the fcc conventional unit cell and the three others at the centers of the adjacent faces (empty in Fig. 2.20a). We thereby construct a crystal with simple cubic Bravais lattice of side  $a$  and a basis of 4 atoms per cell.

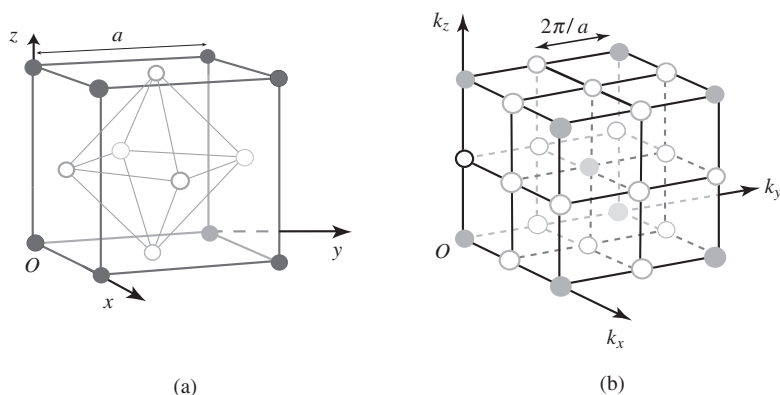


**Fig. 2.20** (a) Simple cubic crystal structure of  $\text{Cu}_3\text{Au}$ . Full spheres represent Au and empty spheres Cu. (b) The reciprocal lattice of the fcc structure is the bcc lattice shown by full spheres. Empty spheres represent the extra reciprocal space nodes which appear for the ordered cubic structure of  $\text{Cu}_3\text{Au}$

There are therefore two simple possibilities, those corresponding to  $\text{Au}_3\text{Cu}$  or  $\text{Cu}_3\text{Au}$ , i.e.,  $x = 0.25$  or  $x = 0.75$ . Naturally, we can imagine ordered solutions for lower concentrations of one of the metals, but there is no particular physical reason why they should ever occur.

Note that, in the ordered  $\text{Cu}_3\text{Au}$  structure, the gold atoms have no Au nearest neighbour. This structure is found to be stable on thermodynamical grounds, which indicates that Au atoms strongly repel one another. However, the  $\text{Au}_3\text{Cu}$  structure is not obtained experimentally, probably because the repulsion between copper atoms is not strong enough. The ordered AuCu alloy exists, but crystallises into a cubic lattice which bears no relation to the fcc structure of the pure metals.

### Question 2.5

The ordered arrangement of the Au and Cu atoms can be detected by a diffraction method. The fcc structure of the disordered solid solution has a primitive cell of volume  $a^3/4$  and a reciprocal lattice with a body-centered cubic conventional cell of side  $4\pi/a$ . The ordered lattice of  $\text{Cu}_3\text{Au}$  shown in Fig. 2.20a has a cubic primitive cell of volume  $a^3$ , and its reciprocal lattice is cubic with side  $2\pi/a$ . There are therefore many diffraction spots for the ordered alloy. In Fig. 2.20b, the lattice points of the body-centered cubic reciprocal lattice are represented by full spheres, while the extra nodes of the simple cubic lattice are represented by empty spheres. The presence of order can thus be revealed by the appearance of diffraction spots associated with these new vectors in reciprocal space.

### Question 2.6

1. The  $C_{60}$  lattice is face-centered cubic with conventional unit cell of side  $a$ . Its reciprocal lattice is body-centered cubic with conventional cell of side  $4\pi/a$  (see Fig. 2.20b). Spots are therefore expected for

$$\mathbf{K} = h\mathbf{a}^* + k\mathbf{b}^* + \ell\mathbf{c}^*, \quad (2.28)$$

with  $|\mathbf{a}^*| = |\mathbf{b}^*| = |\mathbf{c}^*| = 2\pi/a$  and  $h, k, \ell$  of the same parity. In the observed plane of the reciprocal lattice, the spots form a square lattice. The only planes of the body-centered cubic reciprocal lattice with this property are the planes passing through one of the faces of the cube, i.e.,  $(a^*, b^*)$ , or  $(b^*, c^*)$ , or  $(c^*, a^*)$ . Assuming that this is the plane  $(a^*, b^*)$ , the  $a^*$  and  $b^*$  axes are shown in Fig. 2.21. The spots correspond to the vectors  $\mathbf{K} = (h, k, 0)$  with  $h$  and  $k$  even. If  $\ell_{K_0}$  is the spacing of the observed square lattice which corresponds to  $K_0 = 4\pi/a$ , it follows that

$$\frac{4\pi}{a} = \frac{2\pi}{\lambda} \frac{\ell_{K_0}}{L}, \quad \text{and then } a = 2\lambda \frac{L}{\ell_{K_0}}. \quad (2.29)$$

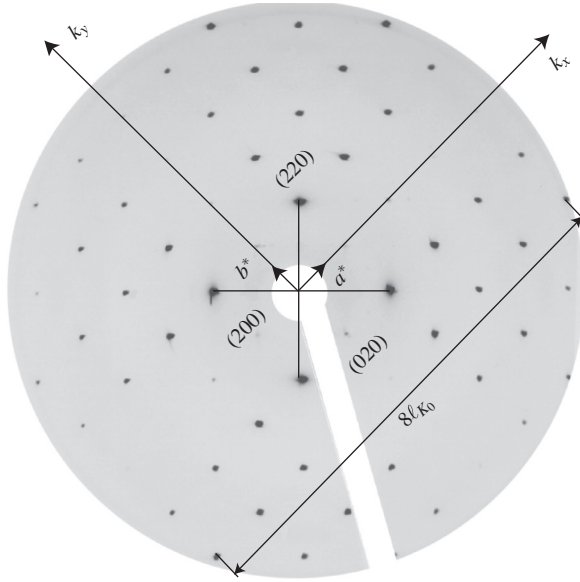


**Fig. 2.21** Indexation of the reciprocal lattice plane of the  $C_{60}$  crystal detected by X-ray diffraction (image on p. 24). See answer to Question 2.6

By measuring over various rows corresponding to 8 times the lattice spacing, and knowing that the film diameter is 12 cm, we obtain  $8\ell_{K_0} = 10.45 \pm 0.05$  cm in Fig. 2.21, so finally,

$$\boxed{a = 14.17 \pm 0.07 \text{ \AA}}. \quad (2.30)$$

2. Note that the spots  $(h,0,0)$  and  $(0,k,0)$  are rather faint. In fact their intensity is found to be at least  $10^3$  times lower than the intensity of the spots  $(220)$ . Set  $\rho(r) = A\delta(r-R)$ . The total number of electrons is 360 per  $C_{60}$ . Hence,

$$360e = \int \rho(r) d^3r = \int_0^\infty 4\pi r^2 \delta(r-R) A dr = A4\pi R^2,$$

which yields

$$A = \frac{360e}{4\pi R^2}.$$

Then

$$\begin{aligned} S(\mathbf{K}) &= \int \rho(r) e^{i\mathbf{K} \cdot \mathbf{r}} d^3r \\ &= \frac{360e}{4\pi R^2} \int_0^\infty r^2 \delta(r-R) dr \int_0^{2\pi} d\phi \int_0^\pi e^{iKr \cos\theta} \sin\theta d\theta \end{aligned}$$

$$\begin{aligned}
&= \frac{360e}{2R^2} \int_0^\infty 2 \frac{\sin Kr}{Kr} r^2 \delta(r-R) dr \\
&= 360e \frac{\sin KR}{KR},
\end{aligned}$$

and the spots have intensity

$$I \propto \frac{\sin^2 KR}{(KR)^2}. \quad (2.31)$$

The intensity vanishes for  $KR = n\pi$  with  $n$  integer. The fact that the spots corresponding to  $K = n(4\pi/a)$  are almost extinguished thus shows that  $4\pi R/a \simeq \pi$ , and then  $R \sim a/4$  or  $R \simeq 3.54 \text{ \AA}$ . With a relative intensity of  $10^{-3}$  for the spot (200) compared with the spot (220), the error obtained for  $R$  is found to be

$$R = 3.54 \pm 0.04 \text{ \AA}. \quad (2.32)$$

In fact, using (2.31) and taking into account the measured intensities for all the spots, the error in  $R$  is much lower, namely  $R = 3.52 \pm 0.01 \text{ \AA}$ .

Introduction to the Physics of Electrons in Solids

Alloul, H.

2011, XXVI, 618 p., Hardcover

ISBN: 978-3-642-13564-4